Modeling and Construction of Single-Wire Power Transmission Based on Multilayer Tesla Coil

Xin Jin, Xiyou Chen, Chen Qi, *Member, IEEE*, and Xianmin Mu

***Abstract*—A single-wire power transmission (SWPT) system based on a multilayer Tesla coil is studied in this article. In the existing SWPT system, a single-layer Tesla coil is usually used, and the maximum transmission efficiency is only 50%–60% within a transmission distance of tens of meters. In this article, a Tesla coil with a multilayer structure is proposed, and the connection of earth also enables the energy of the electromagnetic field to be concentrated, which can greatly improve the transmission efficiency. Moreover, considering the parasitic parameters of the multilayer coil, the circuit model of the Tesla coil is established, and the lumped parameter circuit model of the SWPT system is further obtained. Design guidance is given based on the established model. Long-distance experimental platforms have been built, and various characteristics of the SWPT system, such as input impedance and output power, are studied. In the experiments, when the transmission distance is 70 m, power of 1150 W is transmitted with an efficiency of 90%. Power of 5 kW is transmitted with an efficiency of 87% at a transmission distance of 5 km.**

***Index Terms*—Design, modeling, single-wire power transmission (SWPT), Tesla coil.**

I. Introduction

IN INDUSTRIAL applications, the transmission of electrical energy is achieved through at least two wires. About a hundred years ago, wireless power transmission (WPT) was proposed by Tesla [1], [2]. However, it is difficult for WPT to efficiently transmit large amounts of power over long distances [3], [4], [5], [6], [7]. Therefore, single-wire power transmission (SWPT) has gradually attracted the attention of many researchers.

Greater power can be transmitted by SWPT with higher efficiency over longer distances compared to WPT. SWPT has application prospects in renewable energy systems that supply power to areas far away from the grid, such as rural areas, grasslands, or isolated islands on the sea. This is because in renewable energy systems, such as photovoltaics and wind power, the output voltage is usually dc or low-frequency ac. When SWPT is applied in these scenarios, not only is the power conversion link not added, but also the loss on the line is reduced due to the resonance principle, which saves the investment and operation cost of the transmission line [8]. Moreover, once a line fault occurs, the resonance state of the system will be destroyed, and no more power will be transmitted on the transmission line at that time, thereby avoiding the occurrence of large-scale safety accidents, such as fire and discharge. In addition, the operating frequency of the SWPT system is much higher than that of the current power grid, making it possible to realize half-wavelength power transmission in practical applications. The single wire in the system can also be replaced by other conductive media to improve the flexibility of the power supply. Wireless power transfer for sensors in buildings, trains in mines, and ships on water can be realized when the single wire is replaced by other media, such as metal or water [9].

The SWPT system was first proposed by Tesla [10]. In his patent, the secondary coil of the transformer is connected to the transmission line at one end, and the other end is grounded and connected to the primary coil. In 2001, Strebkov introduced the SWPT system based on the Tesla transformer [11]. A Tesla transformer is used to boost the high-frequency voltage on the transmitting side, and the other transformer on the receiving side converts the high-frequency high-voltage into the voltage and frequency of ordinary electrical appliances. The lumped parameter circuit model of the SWPT system is built in [12], [13], [14], and [15]. In models with Tesla coils, a coil is equivalent to a mutual inductance model. However, in the power transfer experiments over longer distances, the wire lengths of the coils used are usually very long so that the influence of the distributed parameters should be considered. In [16], the coil is described as a long line with distributed parameters. The distributed parameter circuit model of the SWPT system is established in [17]. Whether it is a lumped parameter circuit model or a distributed parameter circuit model, these researchers believe that the loop of the system is completed by the coupling capacitance between the transmitting side and the receiving side. Inevitably, as the transmission distance increases, the coupling becomes weak or even nonexistent. Therefore, based on the electromagnetic field theory, Jin et al. [18] revealed the principle of SWPT at long distances from the theory of electromagnetic surface waves. In [19], it is stated that the single wire belongs to the open waveguide.

In addition to theoretical studies, these researchers also conducted experiments on the SWPT system. In 2017, power of 40 W was transmitted with 66.7% efficiency at 2 m [13]. A nonlinear parity-time symmetric model was proposed in 2018.

Manuscript received 3 September 2022; revised 2 December 2022; accepted 17 January 2023. Date of publication 20 January 2023; date of current version 10 March 2023. This work was supported by the National Natural Science Foundation of China under Grant 51877025. Recommended for publication by Associate Editor R. Hui. *(Corresponding author: Chen Qi.)*

The authors are with the School of Electrical Engineering, Dalian University of Technology, Dalian 116024, China (e-mail: dutjinxin@mail.dlut.edu.cn; chenxy@dlut.edu.cn; qichen@dlut.edu.cn; muxm@dlut.edu.cn).

Color versions of one or more figures in this article are available at https://doi.org/10.1109/TPEL.2023.3238469.

Digital Object Identifier 10.1109/TPEL.2023.3238469

TABLE I
COMPARISONS OF DIFFERENT SWPT SYSTEMS

References	[12]	[17]	[18]	[20]	[22]	**This paper**
Types of coils	Lumped parameter L	Single-layer Tesla coil	Single-layer Tesla coil	Planar coil	Solenoid coil	**Multilayer Tesla coil**
Turns of coils	/	2600	2600	10	915	**1225**
Position of single-wire	Bottom	Bottom	Bottom	Middle	Bottom	**Top**
Earth connections	No	No	No	No	Yes	**Yes**
Operating Frequency	847 kHz	33.8 kHz	34.2 kHz	10.55 MHz	260 kHz	**6.7 kHz**
Transmission Distance	2 m	70 m	100 m	5 m	1.5 m	**5000 m**
Transmission Power	192.6 W	300 W	300 W	65 W	0.5 W	**5000 W**
Transmission Efficiency	61.1%	42%	41.1%	70%	80%	**87%**

Under different transmission distances, the system can reach a stable state, and within the transmission distance of 34 m, the transmission efficiency has always been 60% [14]. In 2021, transmission power can reach 300 or 135 W at transmission distances of 100 or 200 m, respectively [18]. For indoor power supply scenarios, a SWPT method is proposed in [20]. Based on the SWPT system, Van Neste conducted an experimental study using seawater and a single wire to form a composite single-wire. When the transmission distance is 20 m, power of 25 W is transmitted with an efficiency of 54% [21]. In [22], the single wire is replaced by earth to distribute power over a wide area. To improve the transmission efficiency, the effects of inductance and capacitance in the SWPT system were investigated in [23], and power loss of the multiconverter system with single-wire transfer is studied in [24]. Some scholars have proposed a single-wire capacitive power transfer system, in which a single wire is replaced by a capacitor [25], [26], [27]. It has been found in [25] and [26] that this system has a strong ability to resist the lateral and angular deviation of the polar plate, but the transmission power and transmission distance are very small. A single-wire capacitive WPT system with strong coupling to ground is proposed in [27], in which a coupled plate and a single wire are used to generate displacement currents to ground. The system eventually lights up four LEDs for a total output of 3.6 W. Taking advantage of the properties of the self-capacitance of metal objects, a novel WPT system with a single coupling capacitor is proposed in [28]. A detailed circuit model is established, and the final system achieves a power transmission of 20 W with an efficiency of 19.5% at 55 cm.

In the SWPT systems presented in [13], [14], [15], [16], [17], and [18], the high-voltage coils of Tesla coils are all single-layer structures. Moreover, in these structures, the low-voltage coil and the high-voltage coil are loosely coupled, which makes the energy dispersive in the surrounding space relatively strong, resulting in a decrease in transmission efficiency. In the existing experimental research, the maximum transmission efficiency of SWPT within a transmission distance of tens of meters is about 50%–60%. Therefore, in order to further improve the transmission efficiency of the SWPT system, a multilayer Tesla coil is proposed in this article. In the proposed structure, the spacing between layers is extremely small to increase the coupling coefficient of the coils. Also, the earth is connected to the system so that the electromagnetic field energy is concentrated around the system. Various parasitic parameters of the coil are considered, an accurate circuit model of the multilayer Tesla coil is established, and then the lumped parameter circuit model of the whole system is obtained. In the outdoor experiments, when the transmission distance is 70 m, the transmission efficiency can reach 90%, and the transmission efficiency can reach 87% when the transmission distance is 5 km.

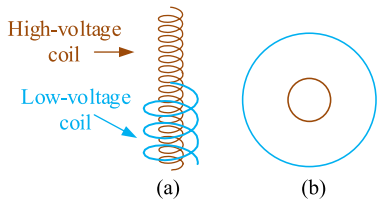

Fig. 1. Single-layer Tesla coil. (a) Front view. (b) Top view.

II. SWPT SYSTEM

At present, SWPT systems with different structures have been studied in some papers. In Table I, the comparison between the existing SWPT systems and the SWPT system studied in this article is presented. In existing SWPT systems, the types of coils used mainly include planar coils, lumped parameter inductors L, solenoid coils, and single-layer Tesla coils. The earliest SWPT system using planar coils was proposed by Tesla [10], but the experimental research work was not carried out by him. Moreover, the magnetic field energy generated by a planar coil is also direction sensitive and decays rapidly with increasing distance. Although the use of a lumped inductor L can reduce the size of the system, the electromagnetic field energy generated by its resonance with the lumped capacitor is limited, so it is not suitable for long-distance power transmission. In order to increase the transmission distance, solenoidal coils or single-layer Tesla coils have been applied in [17], [18], and [22]. As shown in Table I, in these coils, the number of turns is greatly increased, which reduces the operating frequency of the system, thereby reducing the switching loss of the converter. The number of turns of the Tesla coil refers to the number of turns of the high-voltage coil. In a single-layer Tesla coil, as shown in Fig. 1, the height of the low-voltage coil is lower than that of the high-voltage coil, and there is a large air gap between them. Both result in a low coupling coefficient for a single-layer coil. A large part of the energy provided by the power supply will be dissipated into the air.

In experiments, in SWPT systems using planar coils or lumped parameter L, power can only be transferred over a

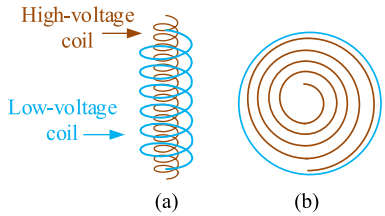

Fig. 2. Multilayer Tesla coil. (a) Front view. (b) Top view.

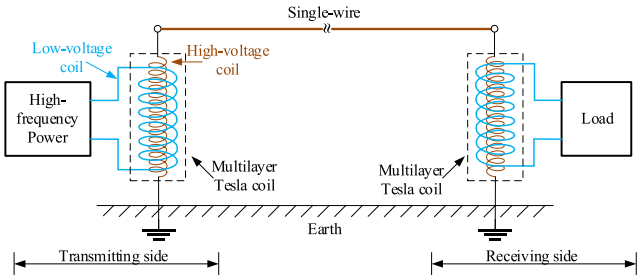

Fig. 3. SWPT system.

distance of a few meters. Although the use of a single-layer Tesla coil can increase the transmission distance and the power of 300 W can be transmitted at 100 m, the transmission efficiency cannot exceed 50% due to the loosely coupled structure of the single-layer coil. The efficiency of the solenoid coil can reach 80% within a transmission distance of 1.5 m, but the efficiency drops significantly after the distance increases. Therefore, in order to improve the transmission efficiency of the system over long distances, a multilayer Tesla coil is proposed in this article, and its structure is shown in Fig. 2. The high-voltage coil is wound in multiple layers, and the low-voltage coil is wound tightly against the outermost layer of the high-voltage coil. Also, the heights of the low-voltage coil and the high-voltage coil are almost the same. There is almost no air gap between the layers of the coil, so the coupling coefficient is greatly increased. When the power supply is connected to the low-voltage coil, the magnetic field generated by it completely passes through the high-voltage coil, reducing the leakage of energy so that the transmission efficiency can be greatly improved.

In the SWPT system, the power transmitting side and the power receiving side are connected by only a single wire. In existing systems, the single wire is mostly located at the bottom of the system. At this time, the electric field is easy to spread so that some low-power devices around the system can receive power wirelessly, and the single wire can also be replaced by some good conductive medium to realize quasi-WPT. However, this method also reduces the power received by the receiving side. In this article, the single wire is at the top of the system, the voltage on the wire is high, and the energy directivity is strong. Moreover, the connection of earth gathers the energy between the single wire and earth, and the energy can be directedly transmitted from the transmitting side to the receiving side, reducing the leakage to surrounding space.

Finally, the SWPT system studied in this article is shown in Fig. 3. Multilayer Tesla coils are used in the system to transform the voltage.

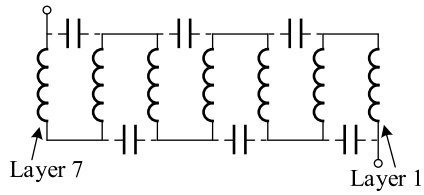

Fig. 4. U-shaped structure.

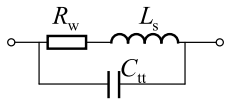

Fig. 5. Circuit model of one layer of the high-voltage coil.

On the transmitting side, the electrical energy provided by the high-frequency power supply is converted into high-frequency high-voltage electrical energy by the Tesla coil. On the receiving side, the high-voltage electrical energy is converted into lower-voltage electrical energy to supply power to the load. The structural parameters of the coils on the transmitting side and the receiving side are the same. The upper ends of the high-voltage coils of the Tesla coils are connected by an overhead single wire. The lower ends of the high-voltage coils are connected to the nearby earth.

III. Modeling

A. Circuit Model of Tesla Coil

The model of the Tesla coil should be built first to obtain the model of the SWPT system. A multilayer Tesla coil is used in this system. The high-voltage coil is wound with seven layers on a cylindrical polyvinyl chloride (PVC) skeleton in a U-shaped structure as shown in Fig. 4. The low-voltage coil is wound close to the outermost layer of the high-voltage coil. In order to ensure good insulation performance between layers, two layers of green-shell insulating paper are wrapped between the layers of the high-voltage coil, and three layers of green-shell insulating paper are wrapped between the low-voltage coil and the high-voltage coil.

Since in a multilayer Tesla coil, each layer of the high-voltage coil has the same physical structure, the circuit model of a layer can be built first. In one layer, the magnetic flux passes through each turn of the coil instantaneously, so a lumped parameter circuit can be modeled with the coil's inductance, resistance, and interturn capacitance, as shown in Fig. 5.

In Fig. 5, R_w, L_s, and $C_{\rm tt}$ are the resistance, self-inductance, and interturn capacitance of one layer, respectively. It should be noted that the operating frequency of the SWPT system is usually tens of kilohertz. In order to make the circuit model more accurate, the skin effect of the wire also needs to be considered. The biggest difference between the multilayer Tesla coil and the single-layer Tesla coil is the existence of interlayer mutual inductance and interlayer capacitance. Moreover, the close interlayer distance of the multilayer coil leads to a large mutual inductance value between layers, and the large number of turns in each layer leads to a large interlayer capacitance.

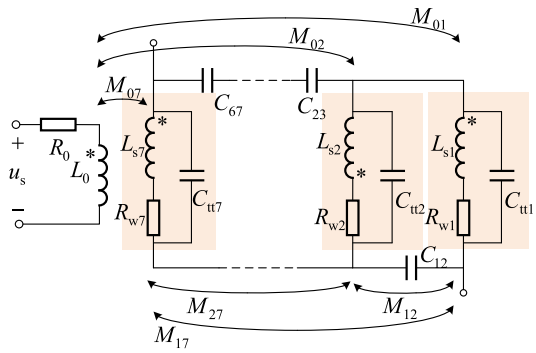

Fig. 6. Circuit model of Tesla coil.

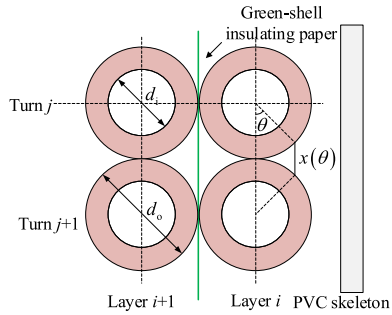

Fig. 7. Basic unit for the high-voltage coil.

Therefore, the circuit model of the multilayer Tesla coil can be described as shown in Fig. 6. In general, the low-voltage coil of the Tesla coil has a small number of turns and a large turn spacing. The circuit model of the low-voltage coil can be represented as a resistor R_0 and an inductor L_0 in series. R_{w1}, $R_{w2}, \ldots, R_{w7}$ are the resistances of each layer of the high-voltage coil. L_{s1}, $L_{s2}, \ldots, L_{s7}$ represent the self-inductances of each layer of the high-voltage coil. $C_{\mathrm{tt}1}$, $C_{\mathrm{tt}2}, \ldots, C_{\mathrm{tt}7}$ are the interturn capacitances of each layer of the high-voltage coil. $C_{12}, C_{23}, \ldots, C_{67}$ represent the capacitances between layers of the high-voltage coil. $M_{01}, \ldots, M_{07}$ are the mutual inductances between each layer of the high-voltage coil and the low-voltage coil. $M_{12}, \ldots, M_{17}$ denote layer-to-layer mutual inductances of the high-voltage coil.

For one layer of coil, the impedance of the wound conductor is given as follows [29]:

$$Z_w \approx R_{w\mathrm{dc}} F \frac{\sinh(2F)+\sin(2F)}{\cosh(2F)-\cos(2F)} + j\frac{\omega\mu l_w}{3\pi} = R_w + j\omega L_w \tag{1}$$

$$F = \left(\frac{\pi}{4}\right)^{0.75} \frac{d_i}{d_{\mathrm{sd}}}\sqrt{\frac{d_i}{p}} \tag{2}$$

where $R_{w\mathrm{dc}} = l_w/\sigma_w S_w$ is the dc resistance of the winding. l_w and S_w denote the length and the cross-sectional area of each layer of the wire, respectively. p represents the turn pitch. $\sigma_w = 5.8 \times 10^7 \mathrm{S/m}$ and $\mu \approx 1.257 \times 10^{-6} \mathrm{H/m}$ are the conductivity and magnetic permeability of the wire, respectively. d_i represents the inner diameter of the wire, $d_{\mathrm{sd}} = 1/\sqrt{\pi f \sigma_w \mu}$ is skin depth. f denotes the operating frequency of the circuit, and $\omega = 2\pi f$ is the angular frequency.

According to (1), the wire resistance R_w and the inductance L_w caused by the energy stored in the wire of one layer of the coil can be obtained as follows:

$$R_w = R_{w\mathrm{dc}} F \frac{\sinh(2F)+\sin(2F)}{\cosh(2F)-\cos(2F)} \tag{3}$$

$$L_w = \frac{\mu l_w}{3\pi}. \tag{4}$$

The inductance of a layer of the coil is determined by the energy stored in the wire and the energy stored in the core of the coil. The inductance L_c due to the energy stored in the core of the coil is given as follows:

$$L_c = \mathrm{K_N}\mu_0 N_m^2 S_c / l_c \tag{5}$$

where N_m represents the number of turns of each layer of the coil, and $\mu_0 = 1.257 \times 10^{-6} \mathrm{H/m}$ is the magnetic permeability in vacuum. S_c and l_c are the cross-sectional area and the length of the coil, respectively. $\mathrm{K_N}$ denote the Nagaoka coefficient. The inductance of the coil will vary depending on the shape of the coil, and this coefficient is a correction factor for the coil

$$\mathrm{K_N} \approx 1/\left[1 + 0.45 D_c/l_c - 0.005 (D_c/l_c)^2\right] \tag{6}$$

where D_c is the diameter of the coil.

Therefore, the total self-inductance of a layer of the coil can be described as follows:

$$L_s = L_c + L_w = \frac{\mathrm{K_N}\mu_0 N_m^2 S_c}{l_c} + \frac{\mu l_w}{3\pi}. \tag{7}$$

Newman's formula is usually used to obtain the mutual inductance between layers. However, due to the large number of turns in each layer of the coil, a large amount of computation occurs. Moreover, since the diameter of the coil in this article is close to the height of the coil, the approximate solution will also bring a large error. Therefore, the mutual inductance parameters in Fig. 6 are obtained by Ansys simulation.

In order to calculate the interturn capacitance and interlayer capacitance in Fig. 6, a basic unit of the high-voltage coil is drawn, as shown in Fig. 7. d_i and d_o are the inner diameter and the outer diameter of the wire, respectively.

In the basic unit of Fig. 7, the interlayer capacitance is composed of the capacitance of the wire insulation layer dC_{sl}, the capacitance of the air gap dC_{air}, and the capacitance of the green-shell insulating paper dC_{hp}. At unit angle $d\theta$, these capacitances can be expressed as follows:

$$dC_{\mathrm{sl}} = \varepsilon_{r1}\varepsilon_0 d\theta \int_0^{l_t} dl \int_{d_i/2}^{d_o/2} \frac{r}{dr} = \frac{\varepsilon_{r1}\varepsilon_0 l_t}{\ln(d_o/d_i)} d\theta \tag{8}$$

$$dC_{\mathrm{air}} = \frac{\varepsilon_0 dS}{x(\theta)} = \frac{\varepsilon_0 l_t d_o}{2x(\theta)} d\theta \tag{9}$$

$$dC_{\mathrm{hp}} = \frac{\varepsilon_{r2}\varepsilon_0 dS}{d_{\mathrm{iso}}} = \frac{\varepsilon_{r2}\varepsilon_0 l_t d_o}{2 d_{\mathrm{iso}}} d\theta \tag{10}$$

where $\varepsilon_{r1} = 3$ and $\varepsilon_{r2} \approx 2$ are the relative permittivities of the insulation layer and green-shell insulating paper, respectively. $\varepsilon_0 = 8.854 \times 10^{-12} \mathrm{F/m}$ represents the permittivity in vacuum,

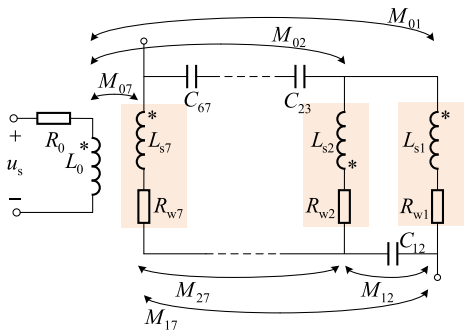

Fig. 8. Simplified model of Tesla coil.

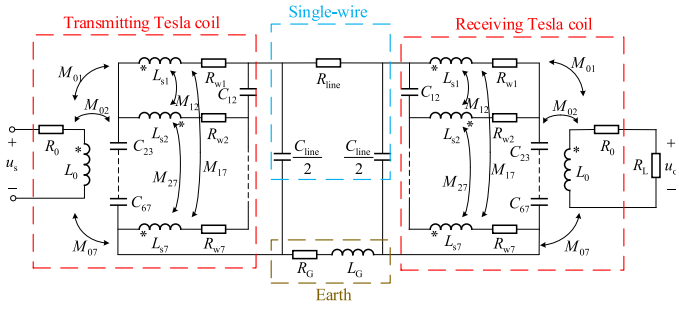

Fig. 9. Model of the SWPT system.

l_t denotes the length of one turn in the coil. d_{iso} represents the thickness of the insulating paper. $x(\theta)$ is the length of the path of the electric field lines in the air. Assuming that the conductor surface is an equipotential surface, the electric field lines between coil turns always propagate along the shortest path, and we can get $x(\theta) \approx [d_o(1-\cos\theta)+1](\text{mm})$. It should be noted that when the coil is wound, it is inevitable that there is a small air gap between the green-shell insulating paper and the coil, resulting in an extra 1mm of error correction in $x(\theta)$.

The interlayer capacitance per unit angle $d\theta$ is the series connection of the capacitance of the wire insulation layer, the capacitance of the air gap, and the capacitance of the green-shell insulating paper. It can be derived as follows:

$$\frac{1}{dC_{\text{ll}}} = \frac{2}{dC_{\text{sl}}} + \frac{1}{dC_{\text{air}}} + \frac{1}{dC_{\text{hp}}}. \tag{11}$$

The interlayer capacitance can be equivalent to the parallel connection of N_m capacitors C_{ll}. Therefore, $C_{12}, C_{23}, \ldots, C_{67}$ in the circuit model presented in Fig. 6 can be obtained as follows:

$$C_{i,i+1} = N_m C_{\text{ll}} = N_m \int_{-\pi/4}^{\pi/4} dC_{\text{ll}}. \tag{12}$$

Compared with the interlayer capacitance, the interturn capacitance is the series connection of $N_m - 1$ basic capacitances, which can be calculated as follows:

$$C_{\text{tti}} = \frac{C_{\text{ttb}}}{N_m - 1} = \frac{\int_{-\pi/4}^{\pi/4} dC_{\text{ttb}}}{N_m - 1} \tag{13}$$

where C_{ttb} denote the basic capacitance between one turn and one turn. Comparing (12) and (13), it can be found that the equivalent value of the interturn capacitance will be much smaller than the interlayer capacitance value. Ignoring the interturn capacitance, the simplified circuit model of the multilayer Tesla coil is shown in Fig. 8.

B. Model of the SWPT System

After obtaining the model of the Tesla coil, the circuit model of the SWPT system is shown in Fig. 9.

Since the structures of the Tesla coils on the transmitting side and the receiving side are the same, the parameters in the circuit model of the transmitting side and the receiving side are also the same.

In the system, the length of the single wire is usually much smaller than the wavelength of the electromagnetic wave corresponding to the operating frequency of the system. Therefore, the transmission line effect of the single wire is ignored, and the wire can be equivalent to a resistance R_{line}. In addition to this, the capacitance of the overhead single-wire to earth also needs to be considered. It is assumed that the erection height of the single wire is much larger than the inner diameter of the wire. The capacitance can be described as follows:

$$C_{\text{line}} = \frac{2\pi\varepsilon_0 l_{\text{line}}}{\ln(2h/a)} \tag{14}$$

where l_{line} represents the length of single wire, and h and a denote the erection height and the radius of the wire, respectively.

R_G and L_G denote the equivalent resistance and equivalent inductance of the earth, respectively. In different regions and different environments, the situation of the earth is very complex, and it is difficult to accurately obtain various parameters of the earth using the analytical method. In this article, the resistance and inductance of the earth are measured experimentally.

IV. Analysis of the Earth

Although energy transmission can be realized in the SWPT system without an earth connection, it can be found from the study of Poynting vector distribution in [18] that a part of the energy is transmitted to the receiving side in the form of electromagnetic surface waves, and a large portion of the energy is dissipated in the surrounding space of the system. The dissipated energy reduces the transmission efficiency of the system. In [18], when the transmission distance is 100 m, the transmission efficiency is 41%, and when the transmission distance is 200 m, the efficiency is only 23%.

The earth is easy to get, and it can be easily connected by simply connecting one end of the Tesla coil to the ground pin inserted into the earth, as shown in Fig. 10. The connection to earth does not bring additional transmission lines to the system, so this system is still a SWPT system. The earth is connected to the system in this article to improve the transmission efficiency.

In order to analyze the influence of the earth on the system, the energy flow law of the system after connecting to the earth is analyzed based on the electromagnetic field theory. As shown in Fig. 11, when the system is connected to the earth, it is assumed that a voltage excitation $\dot{U}$ is applied between the single wire

Fig. 10. Grounding diagram of the system.

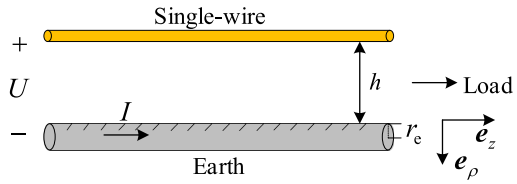

Fig. 11. Single wire and earth in the cylindrical coordinate system.

and earth by the Tesla coil, and the current flowing through the earth is $\dot{I}$.

For the purpose of analysis, Fig. 11 is placed in a cylindrical coordinate system, and the radius of the earth connected to the system is r_e. In the cylindrical coordinate system, the current density in the earth is denoted as follows:

$$\dot{\boldsymbol{J}}(\rho,\phi,z)=\dot{J}_z(\rho)\,\boldsymbol{e}_z. \tag{15}$$

Substituting (15) into the diffusion equation for the current density $\nabla^2\boldsymbol{J}-\sigma_e\mu_e\partial\boldsymbol{J}/\partial t=\boldsymbol{0}$, the scalar equation shown in (16) is obtained

$$\nabla^2\dot{J}_z-j\omega\sigma_e\mu_e\dot{J}_z=0 \tag{16}$$

where σ_e and μ_e are the electric conductivity and the magnetic permeability of the earth, respectively. Equation (16) can be described as follows:

$$\frac{d^2\dot{J}_z}{d\rho^2}+\frac{1}{\rho}\frac{d\dot{J}_z}{d\rho}+k^2\dot{J}_z=0 \tag{17}$$

where $k^2=-j\omega\sigma_e\mu_e$. Moreover, the Bessel equation has the following form:

$$\frac{d^2u}{dx^2}+\frac{1}{x}\frac{du}{dx}+\left(1-\frac{n^2}{x^2}\right)u=0. \tag{18}$$

Comparing (17) and (18), it can be found that (17) is a special case for $n=0$ in (18). Therefore, the current density in the earth is solved according to the general solution of the Bessel equation as follows:

$$\dot{\boldsymbol{J}}=\frac{kI_m}{2\pi r_e}\frac{\mathrm{J}_0(k\rho)}{\mathrm{J}_1(kr_e)}\boldsymbol{e}_z \tag{19}$$

where I_m is the amplitude of the current in the earth. $\mathrm{J}_n(x)$ represents n-order Bessel function of the first kind. The electric field intensity within the earth is given as follows:

$$\dot{\boldsymbol{E}}_{\mathrm{e}}=\frac{\dot{\boldsymbol{J}}}{\sigma_e}=\frac{kI_m}{2\pi\sigma_e r_e}\frac{\mathrm{J}_0(k\rho)}{\mathrm{J}_1(kr_e)}\boldsymbol{e}_z. \tag{20}$$

The effective electric field intensity between the single wire and earth in the $\boldsymbol{e}_\rho$ direction is expressed as follows:

$$\dot{E}_{\rho\mathrm{rms}}=\frac{\dot{U}_{\mathrm{rms}}}{h}. \tag{21}$$

It should be noted that since the ac voltage is between the single wire and earth and the single wire and earth are not symmetrical structures, the electric field intensity distribution between them is time-varying and nonuniform. The introduction of effective electric field strength $\dot{E}_{\rho\mathrm{rms}}$ is just to illustrate the law of energy flow, not for numerical calculation.

According to the boundary condition that the tangential components of the electric field intensity on both sides of the boundary surface are equal, the electric field intensity in the direction of $\boldsymbol{e}_z$ near the earth's surface can be obtained as follows:

$$\dot{E}_z=\frac{kI_m}{2\pi\sigma_e r_e}\frac{\mathrm{J}_0(k\rho)}{\mathrm{J}_1(kr_e)}. \tag{22}$$

The electric field intensity between the wire and earth is given as follows:

$$\dot{\boldsymbol{E}}_{\mathrm{se}}=\dot{E}_{\rho\mathrm{rms}}\boldsymbol{e}_\rho+\dot{E}_z\boldsymbol{e}_z=\frac{\dot{U}_{\mathrm{rms}}}{h}\boldsymbol{e}_\rho+\frac{kI_m}{2\pi\sigma_e r_e}\frac{\mathrm{J}_0(k\rho)}{\mathrm{J}_1(kr_e)}\boldsymbol{e}_z. \tag{23}$$

Using Maxwell's equations and the derivative formula of the Bessel function $\mathrm{J}'_0(z)=-\mathrm{J}_1(z)$, the magnetic field intensity between the wire and earth can be calculated as follows:

$$\dot{\boldsymbol{H}}_{\mathrm{se}}=-\frac{1}{j\omega\mu_0}\nabla\times\dot{\boldsymbol{E}}_{\mathrm{se}}=\frac{\mu_e I_m}{2\pi\mu_0 r_e}\frac{\mathrm{J}_1(k\rho)}{\mathrm{J}_1(kr_e)}\boldsymbol{e}_\phi. \tag{24}$$

The Poynting vector between the single wire and earth is given as follows:

$$\begin{aligned}\boldsymbol{S}=\frac{1}{2}\dot{\boldsymbol{E}}_{\mathrm{se}}\times\dot{\boldsymbol{H}}^*_{\mathrm{se}}&=\frac{\mu_e\dot{U}_{\mathrm{rms}}I_m}{4\pi\mu_0 r_e h}\frac{\mathrm{J}_1^*(k\rho)}{\mathrm{J}_1^*(kr_e)}\boldsymbol{e}_z\\&+\frac{\mu_e kI_m^2}{8\pi^2\mu_0\sigma_e r_e^2}\frac{\mathrm{J}_0(k\rho)\,\mathrm{J}_1^*(k\rho)}{\mathrm{J}_1(kr_e)\,\mathrm{J}_1^*(kr_e)}(-\boldsymbol{e}_\rho).\end{aligned} \tag{25}$$

In (25), the first term of the Poynting vector represents the energy flux density into the load, and the second term is the energy flux density into the earth and single wire. It is concluded from (25) that the electromagnetic field energy excited by the Tesla coil is transmitted to the load through the spatial electromagnetic field between the single wire and the earth. The role of the earth is to gather electromagnetic energy and guide the directional transmission of energy together with the single wire.

In order to compare the effect of whether the earth is connected or not on the energy propagation law in the SWPT system, the simulation model was built in the High Frequency Structure Simulator. The simulation results are shown in Fig. 12. Fig. 12(a) shows the distribution of the Poynting vector in the SWPT system without earth connection, and Fig. 12(b) shows the case with earth connection. When the earth is not connected to the system, part of the Poynting vector points from one coil to another along the single wire, but another part points to infinity, which

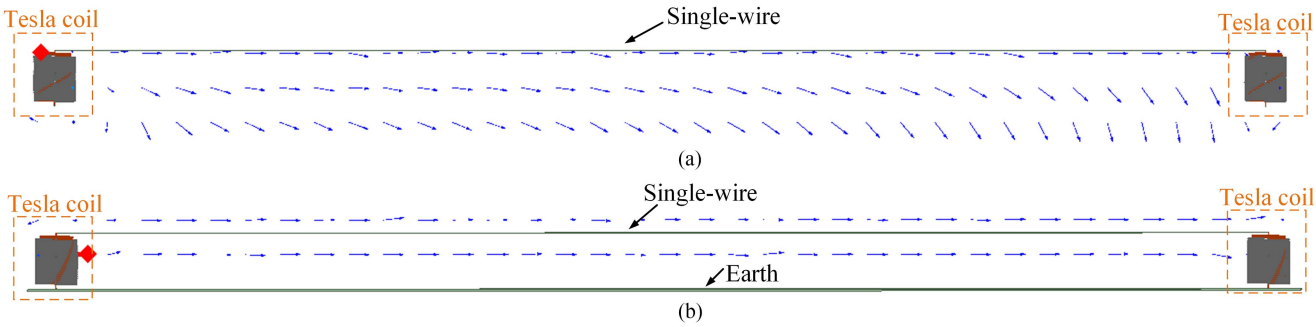

Fig. 12. Distribution of the Poynting vector. (a) No earth connection. (b) With earth connection.

indicates that a large part of the electromagnetic field energy is not received by the load but is dissipated in the surrounding space, which leads to a reduction in the transmission efficiency of the system. When the system is connected to earth, as shown in Fig. 12(b), the electromagnetic field energy is gathered around the single wire and earth. More electromagnetic field energy is transmitted to the load through the guidance of the single wire and earth, so the transmission efficiency can be significantly improved.

V. Design of the SWPT System

The design of the SWPT system mainly has two parts, one is the design of the Tesla coil, and the other is the design of the operating frequency of the system. The design is mainly completed based on the established circuit model shown in Fig. 9.

A. Design of the Tesla Coil

The low voltage provided by the high-frequency power supply can be raised by the coil to a high voltage of kilovolts or even tens of thousands of volts through resonance. In a single-layer coil, the interturn voltage can be easily reduced by increasing the number of turns of the coil, and very thin wires, such as enameled wire, can be used in the coil. However, there are high interlayer voltages in multilayer coils in this article, and the insulation capacity of the wires must be increased to ensure the safe operation of the system. Eventually, a silicone wire with an outer diameter of 4 mm is selected to be wound on a skeleton with a diameter of 400 mm.

The number of turns and layers of the coil should be selected based on the requirements of the transmission performance of the system. When the total number of turns of the coil is constant, the curves of output power and transmission efficiency calculated by the circuit model shown in Fig. 9 with the number of layers are shown in Fig. 13. N_l in the figure represents the number of layers of the coil. When N_l is relatively small, the output power in the system is larger under the same input voltage, but the transmission efficiency is lower. Although the efficiency improvement can be achieved by increasing N_l, the number of turns per layer is reduced, which reduces the output power under the same input voltage, and the excessive number of layers will also increase the volume of the Tesla coil.

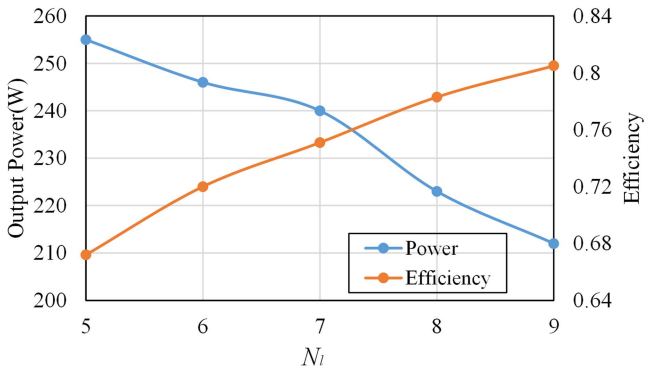

Fig. 13. Power and efficiency versus layers.

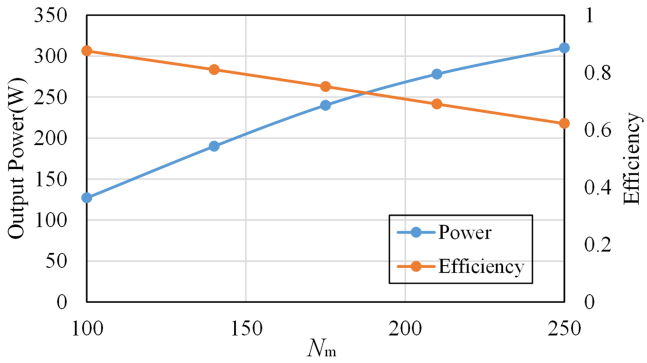

Fig. 14. Power and efficiency versus number of turns.

When N_l is constant, the curves of output power and transmission efficiency calculated by the circuit model in Fig. 9 with the number of turns of each layer are shown in Fig. 14. As shown in Fig. 14, when N_l is constant, the increase in N_m can increase the transmission power of the system. However, too many turns in the coil also bring a lot of copper loss to the system, reducing the transmission efficiency.

Therefore, the number of turns and layers should be determined according to the needs of practical applications. For example, in some low-power applications, the number of layers of the coil can be increased to improve the transmission efficiency. In this article, in the SWPT system that requires long-distance high-power and high-efficiency power transmission, power and efficiency are both important parameters. Therefore,

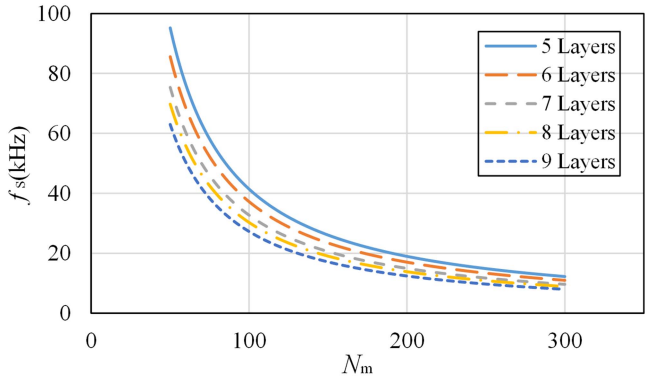

Fig. 15. Relationship between the self-resonant frequency and the number of turns and layers.

Fig. 16. Homemade multilayer Tesla coils.

the influence of N_m and N_l on them needs to be considered comprehensively. Finally, according to Figs. 13 and 14, the number of layers is selected as seven layers, and the number of turns of each layer is 150–200 turns. Six or eight layers are not selected because an even number of layers will cause the highest and lowest potentials in the coil to exist at the top or bottom of the coil at the same time, resulting in higher requirements for the insulation of the wires.

B. Design of Operating Frequency

The operating frequency of the system is close to the self-resonant frequency of the Tesla coil, and the self-resonant frequency depends on the specific parameters of the coil. The self-inductance of one layer of the coil can be obtained by (7). The total equivalent inductance of the multilayer coil is about

$$L_{\text{eq}} \approx N_l L_s + M_{\text{eq}} N_l \left(N_l - 1\right) \tag{26}$$

where M_{eq} is the mutual inductance between layers. In order to simplify the calculation, the parameters of each layer of the coil are homogenized, that is, the self-inductance of each layer is considered to be approximately equal, and the mutual inductance between layers is also approximately equal.

The total equivalent capacitance of the multilayer coil is given as follows [30]:

$$C_{\text{eq}} = \frac{1}{N^2}\left[C_{\text{ttb}}\left(N_m - 1\right) N_l + C_{\text{ll}} \frac{N_m\left(4N_m^2 - 1\right)}{3}\left(N_l - 1\right)\right] \tag{27}$$

where N is the total number of turns of the coil.

The self-resonant frequency of the Tesla coil can be obtained as follows:

$$f_s = \frac{1}{2\pi\sqrt{L_{\text{eq}} C_{\text{eq}}}}. \tag{28}$$

Substituting (26) and (27) into (28), the relationship between the self-resonant frequency and the number of turns and layers of the coil is shown in Fig. 15.

As shown in Fig. 15, the increase in the number of layers and turns of the coil will lead to a decrease in the self-resonant frequency. After determining the transmission scale of the system, the size of the coil can be determined from Figs. 13 and 14, and then the self-resonant frequency of the Tesla coil can be determined from Fig. 15.

TABLE II
SPECIFIC PARAMETERS OF TESLA COIL

	High-voltage coil	Low-voltage coil
Layers	7	1
Height	700 mm	680 mm
Total turns	1225	34
Wire diameter	4 mm	9.2 mm
Cross-sectional area	1.3 mm^2	31.4 mm^2

VI. EXPERIMENTAL RESULTS

A. Experimental Testing of Tesla Coils

In order to enable the SWPT system to achieve high-power and high-efficiency transmission at the same time, according to the circuit model established in Fig. 9 and the influence of N_m and N_l on power and efficiency in Figs. 13 and 14, the number of layers of the Tesla coil in the experiment is finally selected to be seven layers, and the number of turns of each layer is 175 turns. The completed coils are shown in Fig. 16. The specific parameters of the coil are shown in Table II. The height of the low-voltage coil is close to that of the high-voltage coil, and in order to increase the turns ratio between the two, a blue nylon rope with an outer diameter of 10 mm is alternately wound with the low-voltage coil to increase the turn spacing. The green-shell insulating paper with a thickness of 0.5 mm is wrapped between the layers of the coil to increase the insulation strength. The material of the low-voltage coil is Litz wire, and the material of the high-voltage coil is silicone wire.

The resistances, inductances, and capacitances in the circuit model of the Tesla coil can be calculated from the data presented in Table II. The mutual inductance values between layers obtained by Ansys simulation are shown in Table III.

In order to verify the validity of the circuit model of the Tesla coil, the frequency characteristics of the input impedance of a Tesla coil are shown in Figs. 17 and 18 when the high-voltage coil is opened and shorted, respectively. In the experiment, the signal generated by the waveform generator is connected to

TABLE III
MUTUAL INDUCTANCE VALUES BETWEEN LAYERS (UNIT: MH)

M_{01}	1.01	M_{02}	1.06	M_{03}	1.12	M_{04}	1.18
M_{05}	1.23	M_{06}	1.3	M_{07}	1.36	M_{12}	5.34
M_{13}	5.29	M_{14}	5.24	M_{15}	5.2	M_{16}	5.16
M_{17}	5.12	M_{23}	5.57	M_{24}	5.52	M_{25}	5.48
M_{26}	5.43	M_{27}	5.39	M_{34}	5.81	M_{35}	5.76
M_{36}	5.72	M_{37}	5.67	M_{45}	6.05	M_{46}	6
M_{47}	5.95	M_{56}	6.31	M_{57}	6.25	M_{67}	6.56

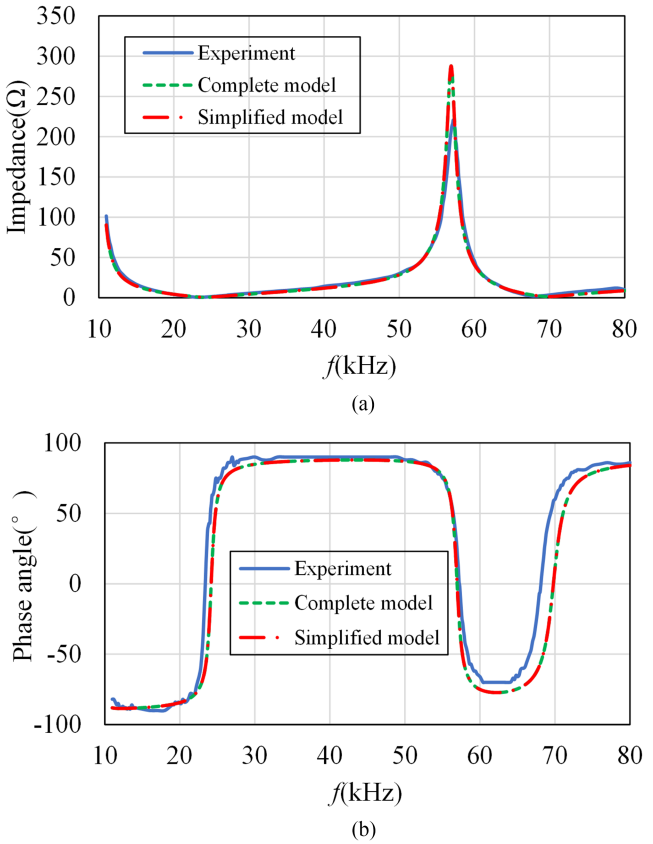

Fig. 17. Frequency characteristics when the high-voltage coil is opened. (a) Amplitude–frequency characteristics. (b) Phase frequency characteristics.

the low-voltage coil of the Tesla coil after being amplified by HSA4011 amplifier. After the voltage and current waveforms of the low-voltage coil are measured by an oscilloscope, the amplitude and phase of the input impedance are obtained. In Figs. 17 and 18, the complete model refers to the circuit model presented in Fig. 6, and the simplified model is the circuit model with the interturn capacitance removed, as shown in Fig. 8.

In Fig. 17, when the high-voltage coil is opened, there are three extreme points in the amplitude–frequency characteristic curve. At the frequencies corresponding to the three extreme points, the errors of the experimental measurement results and the calculation results of the complete model are 2.5%, 0.5%, and 2.8%, respectively. In Fig. 18, when the high-voltage coil is shorted,

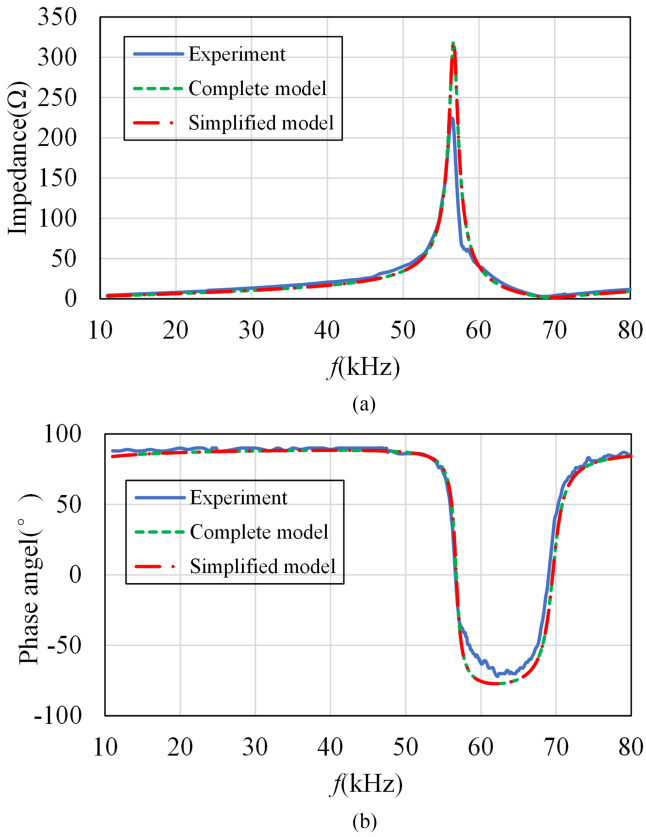

Fig. 18. Frequency characteristics when the high-voltage coil is shorted. (a) Amplitude–frequency characteristics. (b) Phase frequency characteristics.

at the frequencies corresponding to the two extreme points, the errors of the experimental and theoretical calculations are 0.2% and 1.2%, respectively. Regardless of whether the high-voltage coil is shorted or opened, the curve trend of the complete model is consistent with the experimental curve, indicating that the circuit model shown in Fig. 6 is effective. Moreover, in Figs. 17 and 18, the curves of the simplified model and the complete model basically overlap, indicating that the simplification of the circuit model is reasonable. Therefore, when establishing the circuit model of the SWPT system, the simplified circuit model shown in Fig. 8 can be directly used.

B. Experiments of SWPT Systems

A SWPT system is built for doing experimental research. Fig. 19 shows the experimental scene diagram when the transmission distance is 70 m. Fig. 20 shows the experimental schematic diagram of the SWPT system. In the experiment, the upper ends of the high-voltage coils on the transmitting side and the receiving side are connected by an overhead single-wire, and the lower ends are respectively connected to the nearby soil. The material of the single wire is a silicone wire with an outer diameter of 4 mm and a cross-sectional area of 1.3 mm^2. After experimental measurement, the equivalent resistance and equivalent inductance of the earth in the model are $R_G = 110\ \Omega$ and $L_G = 175\ \mu$H, respectively.

Fig. 19. Experimental site with a transmission distance of 70 m. (a) Panoramas. (b) Transmitting side. (c) Receiving side.

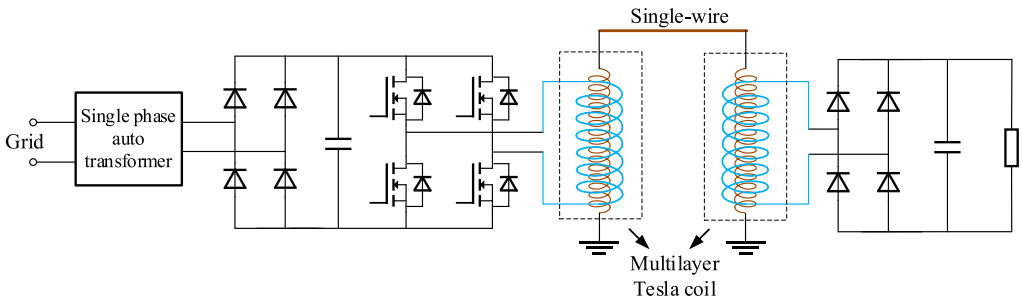

Fig. 20. Experimental schematic diagram of the SWPT system.

The operating frequency range of the system can be roughly estimated from the self-resonant frequency of the coil shown in Fig. 15, and the specific operating frequency needs to be determined according to the established circuit model of the system. When the load resistance is 20 Ω, the frequency characteristics of the input impedance of the SWPT system are shown in Fig. 21. The frequency characteristic curve of the input impedance calculated by the model is basically consistent with the curve measured by the experiment. When the system works at the frequency corresponding to the minimum input impedance amplitude, more power can be transmitted from the transmitting side to the receiving side. In Fig. 21(a), there are two frequencies corresponding to the minimum values of the input impedance amplitude, which are about 16.7 and 66 kHz, respectively. Voltage gain is defined as the ratio of the output voltage on the receiving side to the input voltage on the transmitting side. In theoretical calculations and experimental measurements, the voltage gain at 16.7 kHz is much greater than that at 66 kHz, at which power can hardly be transferred. Therefore, the following studies were carried out at frequencies around 16.7 kHz.

The frequency characteristic curves of voltage gain and output power are shown in Fig. 22. When the operating frequency is about 16.4 kHz, the voltage gain reaches a maximum value of about 2.7. At the same time, at this frequency, the receiving side can also receive the maximum power. In Figs. 21 and 22, the frequency characteristics of the input impedance, voltage gain, and output power calculated by the model of the SWPT system are all consistent with the experimental results, and the agreement between them is extremely high, which verifies that the SWPT system model presented in Fig. 9 is effective and accurate.

Through the analysis of the frequency characteristics of the input impedance and voltage gain, the operating frequency of the SWPT system is selected to be around 16.4 kHz. According to the design results of the SWPT system in Section V, as shown in Fig. 15, the self-resonant frequency of the Tesla coil is about 17.3 kHz, and the error between the experimental results and the design results is 5.5%. The appearance of this error is due to the influence of the single-wire-to-earth capacitance on the operating frequency of the system.

When the operating frequency is 16.4 kHz, as shown in Fig. 19(c), a group of incandescent lamps are lit. When the transmission distance is 70 m, the SWPT system transmits power of 1150 W with an efficiency of 90%.

In the same experimental scenario, when the transmission distance is 70 m, the SWPT system using a single-layer Tesla coil in [17] can only transmit a power of 300 W with an efficiency of 42%. The transmission efficiency of the multilayer coil is much greater than that of the single-layer coil. In [17], when the output power is 300 W, the output current on the transmitting side is close to the safety threshold of the MOSFET, so that the power cannot continue to increase. Although the turns ratio and

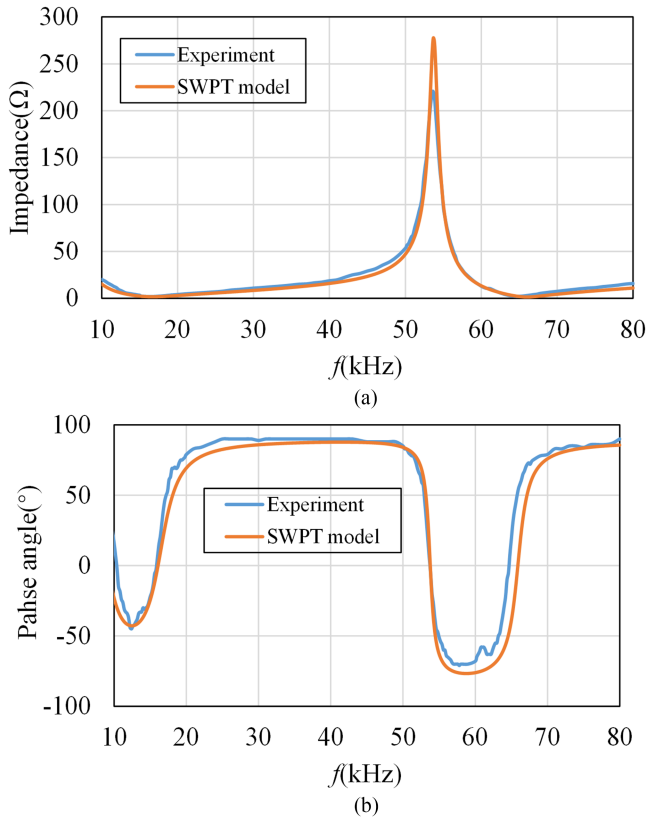

Fig. 21. Frequency characteristics of input impedance of the SWPT system. (a) Amplitude–frequency characteristics. (b) Phase frequency characteristics.

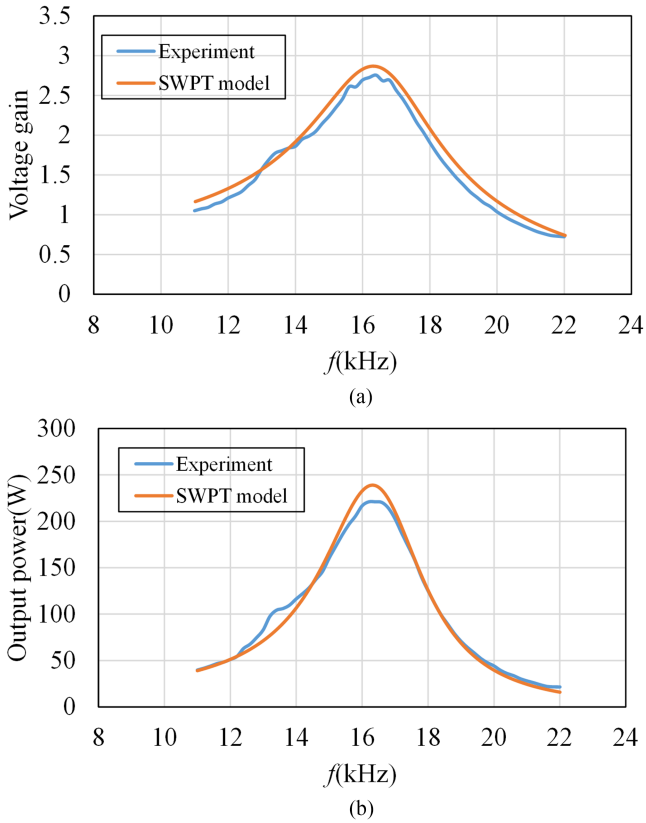

Fig. 22. Frequency characteristics of the SWPT system. (a) Frequency characteristics of voltage gain. (b) Frequency characteristics of output power.

voltage gain of a single-layer coil are greater than those of a multilayer coil, in a multilayer coil, the coupling coefficient is greatly increased due to the close winding between layers. Therefore, compared with the single-layer coil, less energy in the multilayer coil will be dissipated to the surrounding space, so that the transmission efficiency can be greatly improved.

When the output voltage is 120 V, the voltage and current waveforms of the power supply, the current waveforms of the single wire and the earth are shown in Fig. 23.

The earth current and the single-wire current have close magnitude and phase, and the rms value of their current is about 0.47 A. Since this current value is small, very thin wires can be used for a single wire. Compared with traditional power lines, metal materials are greatly saved. Small currents reduce losses to the earth.

To explore the possibility of using multilayer Tesla coils to realize SWPT at longer distances, an experimental platform with a transmission distance of 5 km is established in Shanghai, China, as shown in Fig. 24. In Fig. 24, the multilayer Tesla coil is fabricated in the same way as shown in Fig. 16. The 5-km-long single-wire is arranged in a U shape in the experimental site and is overhead through many PVC pipes.

When the operating frequency is 6.7 kHz, the voltage and current waveforms of the high-frequency power supply are in phase. At this point, the SWPT system transmits power of 5 kW with an efficiency of 87%. As shown in Fig. 25, 35 incandescent lamps rated at 200 W are lit.

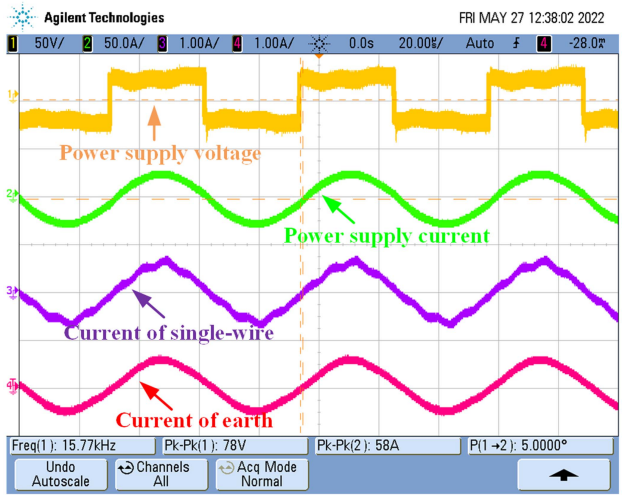

Fig. 23. Waveforms when the output voltage is 120 V.

Compared with the transmission distance of 70 m, the decrease in the operating frequency is due to the increase in the length of the single wire, resulting in the increase in the single-wire-to-earth capacitance.

When the output power on the receiving side is 5 kW, the current waveforms of the single wire and the earth are shown in Fig. 26. The earth current and the single-wire current have close magnitude and phase, and the rms value of their current is about 2.29 A. From the waveforms shown in Figs. 23 and 24, it

Fig. 24. Experimental site with a transmission distance of 5 km.

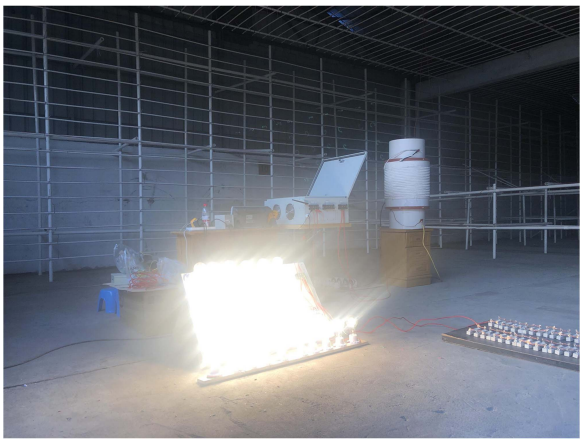

Fig. 25. Power of 5 kW is transmitted at a transmission distance of 5 km.

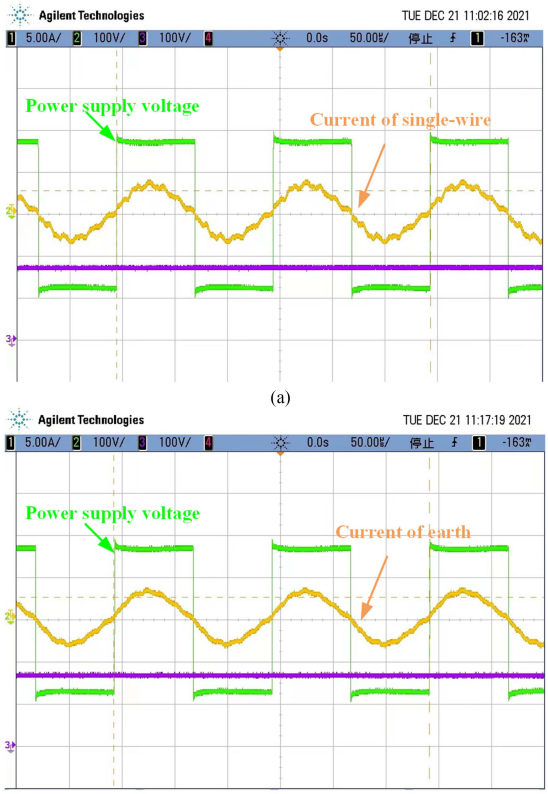

Fig. 26. Current waveforms when the output power is 5 kW. (a) Current of single wire. (b) Current of earth.

can be seen that the waveforms of the single-wire current and the earth current are not exactly the same, and their amplitudes have small differences, which shows that the earth cannot be completely equivalent to a wire. The role of the earth is to gather the energy of the electromagnetic field and guide the directional transmission of energy.

When the transmission distance is 5 km, the resistance on the wire is about 96 Ω, and the power loss on the wire is about 503 W. The loss on the wire is 67.3% of the total loss of the SWPT system. Therefore, reducing the loss on the wire to further improve the efficiency can be the content of future research. Loss can be reduced by increasing the voltage of the Tesla coil to reduce the current or using some low loss wire to reduce the resistance. In addition, the circuit model established in this article can also be used to design the compensation network and the closed-loop control of the SWPT system, which we will study in future.

VII. Conclusion

A SWPT system based on a multilayer Tesla coil structure is studied. The main contributions of this paper are summarized as follows.

1) In order to improve the transmission efficiency of the SWPT system, a multilayer Tesla coil structure is proposed.
2) An accurate circuit model of the SWPT system is established, and the design guidance of the system is also given.
3) In the experiment, when the transmission distance is 5 km, power of 5 kW can be transmitted with an efficiency of 87%, which greatly improves the transmission level of the SWPT system.

Compared with the single-layer coil, the leakage of energy is reduced due to the high coupling coefficient of the multilayer coil. In addition, the connection of the earth also concentrates the electromagnetic field energy between the single wire and earth, and the energy is directed to be transmitted from the transmitting side to the receiving side so that the transmission efficiency of the SWPT system is improved. Considering the parasitic parameters of the coil, the circuit model of the single wire, and the earth, an accurate lumped parameter circuit model of the SWPT system is established. The frequency characteristics of input impedance, voltage gain, and output power are studied. These frequency characteristics are highly consistent with the calculated results of

the model, and the validity of the SWPT system model is verified. According to the influence of various parameters calculated by the model on power and efficiency, the design of the Tesla coil and operating frequency can be completed. In the experiment, power of 1150 W is transmitted with an efficiency of 90% at a transmission distance of 70 m, and power of 5 kW is transmitted with an efficiency of 87% at a transmission distance of 5 km. The change in the transmission distance will cause a change in the single-wire-to-earth capacitance, which will lead to a change in the operating frequency. It is found that when the SWPT system is used for long-distance high-power power transmission, the current on the single wire is very small. Therefore, the single wire can be made with very thin wire to save material, and the small current also leads to lower losses in the SWPT system.

Acknowledgment

The authors would like to thank Shanghai Electric Power New Energy Development Co., Ltd. for providing the experimental site needed for this article.

References

[1] N. Tesla, "The true wireless," *Elect. Experimenter*, vol. 5, pp. 28–32, May 1919.
[2] N. Tesla, "World system of wireless transmission of energy," *Telegraph Telephone Age*, vol. 20, pp. 457–460, Oct. 1927.
[3] Y. Fan, Y. Sun, X. Dai, Z. Zuo, and A. You, "Simultaneous wireless power transfer and full-duplex communication with a single coupling interface," *IEEE Trans. Power Electron.*, vol. 36, no. 6, pp. 6313–6322, Jun. 2021, doi: 10.1109/TPEL.2020.3035782.
[4] X. Tian, K. T. Chau, W. Liu, H. Pang, and C. H. T. Lee, "Maximum power tracking for magnetic field editing-based omnidirectional wireless power transfer," *IEEE Trans. Power Electron.*, vol. 37, no. 10, pp. 12901–12912, Oct. 2022, doi: 10.1109/TPEL.2022.3178097.
[5] L. Huang, A. P. Hu, A. K. Swain, and Y. Su, "Z-impedance compensation for wireless power transfer based on electric field," *IEEE Trans. Power Electron.*, vol. 31, no. 11, pp. 7556–7563, Nov. 2016, doi: 10.1109/TPEL.2016.2557461.
[6] M. Wu, X. Chen, C. Qi, and X. Mu, "Considering losses to enhance circuit model accuracy of ultrasonic wireless power transfer system," *IEEE Trans. Ind. Electron.*, vol. 67, no. 10, pp. 8788–8798, Oct. 2020, doi: 10.1109/TIE.2019.2947802.
[7] M. Wu et al., "Transferring power and data simultaneously of different direction in ultrasonic contactless power transfer system," *Energy Rep.*, vol. 8, pp. 72–80, 2022, doi: 10.1016/j.egyr.2022.02.155.
[8] D. Strebkov et al., "Single-wire resonant electric power systems for renewable-based electric grid," in *Handbook of Research on Renewable Energy and Electric Resources for Sustainable Rural Development*. Hershey, PA, USA: IGI Global, 2018, pp. 449–474.
[9] D. S. Strebkov, A. I. Nekrasov, and A. A. Nekrasov, "Resonant methods for electric power transmission and application," *Machinery Energetics. J. Rural Prod. Res.*, vol. 9, no. 2, pp. 37–43, 2018, doi: 10.31548/me2018.02.037.
[10] N. Tesla, "Electrical transformer," U.S. Patent 593 138, Nov. 2, 1897.
[11] D. S. Strebkov, S. V. Avramenko, and A. I. Nekrasov, "Single-wire electric power system for renewable-based electric grid," *New Energy Technol. Mag.*, vol. 1, pp. 20–25, Jul. 2001.
[12] X. Chen, T. Li, Z. Lang, and C. Qi, "A single-wire power transfer system using lumped-parameter LC resonant circuits," in *Proc. IEEE 9th Int. Power Electron. Motion Control Conf.*, 2020, pp. 1098–1103, doi: 10.1109/IPEMC-ECCEAsia48364.2020.9367764.
[13] X. Chen, J. Chen, G. Li, X. Mu, and C. Qi, "Electric-field-coupled single-wire power transmission—Analytical model and experimental demonstration," in *Proc. IEEE Int. Symp. Power Electron.*, 2017, pp. 1–6, doi: 10.1109/PEE.2017.8171661.
[14] X. Shu and B. Zhang, "Single-wire electric-field coupling power transmission using nonlinear parity-time-symmetric model with coupled-mode theory," *Energies*, vol. 11, no. 3, 2018, Art. no. 532, doi: 10.3390/en11030532.
[15] G. Liu and B. Zhang, "Analytical model of a 25–50 m robust single-wire electric-field coupling power transfer system using a limiter," *IEEE Trans. Circuits Syst. II, Exp. Briefs*, vol. 66, no. 6, pp. 978–982, Jun. 2019, doi: 10.1109/TCSII.2018.2867571.
[16] J. Voitkans and A. Voitkans, "Tesla coil theoretical model and experimental verification," *Elect., Control Commun. Eng.*, vol. 7, no. 1, pp. 11–19, 2014, doi: 10.1515/ecce-2014-0018.
[17] T. Li, X. Chen, Z. Lang, X. Jin, C. Qi, and Y. Wang, "Modeling and analysis of single-wire power transfer system using distributed parameter resonant coil," in *Proc. IEEE Ind. Electron. Appl. Conf.*, 2021, pp. 141–145, doi: 10.1109/IEACon51066.2021.9654728.
[18] X. Jin, X. Chen, C. Qi, and T. Li, "Investigation on the electromagnetic surface waves for single-wire power transmission," *IEEE Trans. Ind. Electron.*, vol. 70, no. 3, pp. 2497–2507, Mar. 2023, doi: 10.1109/TIE.2022.3170634.
[19] Y. Li et al., "Single-wire power transfer method and verification," *J. Power Electron.*, vol. 22, no. 4, pp. 685–693, 2022, doi: 10.1007/s43236-022-00383-4.
[20] Y. Li et al., "A novel single-wire power transfer method for wireless sensor networks," *Energies*, vol. 13, no. 19, 2020, Art. no. 5182, doi: 10.3390/en13195182.
[21] C. W. Van Neste and S. M. Mahajan, "Wireless reactive power transfer for off-shore energy harvesting," in *Proc. IEEE Int. Conf. Clean Elect. Power*, 2009, pp. 504–506, doi: 10.1109/ICCEP.2009.5212003.
[22] C. V. Neste et al., "Electrical excitation of the local earth for resonant, wireless energy transfer," *Wireless Power Transfer*, vol. 3, no. 2, pp. 117–125, 2016, doi: 10.1017/wpt.2016.8.
[23] F. Zhang et al., "Research on the efficiency of single-wire power transmission," *J. Phys., Conf. Ser.*, vol. 2121, no. 1, 2021, Art. no. 012010, doi: 10.1088/1742-6596/2121/1/012010.
[24] M. Zygmanowski et al., "Power loss analysis of multi-converter system with single wire and wireless energy transfer," in *Proc. IEEE Int. Conf. Elect. Drives Power Electron.*, 2021, pp. 206–211, doi: 10.1109/EDPE53134.2021.9604052.
[25] L. J. Zou, A. P. Hu, and Y. Su, "A single-wire capacitive power transfer system with large coupling alignment tolerance," in *Proc. IEEE PELS Workshop Emerg. Technol., Wireless Power Transfer*, 2017, pp. 93–98, doi: 10.1109/WoW.2017.7959372.
[26] L. J. Zou and A. P. Hu, "A contactless single-wire CPT (capacitive power transfer) power supply for driving a variable message sign," in *Proc. IEEE PELS Workshop Emerg. Technol., Wireless Power Transfer*, 2018, pp. 1–5, doi: 10.1109/WoW.2018.8450894.
[27] L. J. Zou, Q. Zhu, C. W. Van Neste, and A. P. Hu, "Modeling single-wire capacitive power transfer system with strong coupling to ground," *IEEE J. Emerg. Sel. Topics Power Electron.*, vol. 9, no. 2, pp. 2295–2302, Apr. 2021, doi: 10.1109/JESTPE.2019.2942034.
[28] X. Gao et al., "Capacitive power transfer through virtual self-capacitance route," *IET Power Electron.*, vol. 11, no. 6, pp. 1110–1118, Mar. 2018, doi: 10.1049/iet-pel.2017.0629.
[29] M. K. Kazimierczuk, *High-Frequency Magnetic Components*, 2nd ed. Hoboken, NJ, USA: Wiley, 2014, pp. 326–335.
[30] B. Wu, X. Zhang, X. Liu, and C. He, "An analytical model for predicting the self-capacitance of multi-layer circular-section induction coils," *IEEE Trans. Magn.*, vol. 54, no. 5, May 2018, Art. no. 6201007, doi: 10.1109/TMAG.2018.2803771.

Xin Jin was born in Hubei, China, in 1995. He received the bachelor's degree in electrical engineering from Shandong Technology and Business University, Yantai, China, in 2017, and the master's degree in electrical engineering in 2020 from the Dalian University of Technology, Dalian, China, where he is currently working toward the Ph.D. degree in power electronics and power transmission.

His research interests include wireless power transfer and power conversion.

Xiyou Chen was born in Heilongjiang, China, in 1962. He received the B.S., M.S., and Ph.D. degrees in electrical engineering from the Harbin Institute of Technology, Harbin, China, in 1982, 1985, and 2000, respectively.

From April 2004 to March 2005, he was a Visiting Scholar with the Department of Electrical and Computer Engineering, University of Waterloo, Waterloo, ON, Canada. He is currently a Professor with the School of Electrical Engineering, Dalian University of Technology, Dalian, China. His research interests include power converters and wireless power transfer.

Chen Qi (Member, IEEE) received the B.Sc. and Ph.D. degrees in electrical engineering from the School of Electrical Engineering, Dalian University of Technology, Dalian, China, in 2009 and 2014, respectively.

From April 2015 to October 2016, he was a Postdoctoral Fellow with the Rolls-Royce@NTU Corporate Lab, Nanyang Technological University, Singapore. Since November 2016, he has been with Dalian University of Technology, Dalian, China, where he is currently an Associate Professor. His research interests include wireless power transfer, multilevel converters, and model predictive control.

Xianmin Mu was born in Heilongjiang, China, in 1973. He received the M.S. and Ph.D. degrees in electrical engineering from the Harbin Institute of Technology, Harbin, China, in 2002 and 2007, respectively.

Since 2013, he has been an Associate Professor with the Department of Electrical Engineering, Dalian University of Technology, Dalian, China. His research interests include power quality, magnetic controllable reactors, and power electronic converters.